Separation Science and Technology
Publication details, including instructions for authors and subscription information:
http://www.informaworld.com/smpp/title~content=t713708471

Separation of Metal Species by Supported Liquid Membranes

Pier R. Danesi[a]
[a] CHEMISTRY DIVISION ARGONNE NATIONAL LABORATORY ARGONNE, ILLINOIS

To cite this Article Danesi, Pier R.(1984) 'Separation of Metal Species by Supported Liquid Membranes', Separation Science and Technology, 19: 11, 857 — 894
To link to this Article: DOI: 10.1080/01496398408068598
URL: http://dx.doi.org/10.1080/01496398408068598

SEPARATION SCIENCE AND TECHNOLOGY, 19(11 & 12), pp. 857-894, 1984-85

Separation of Metal Species by Supported Liquid Membranes

PIER R. DANESI

CHEMISTRY DIVISION
ARGONNE NATIONAL LABORATORY
ARGONNE, ILLINOIS 60439

Abstract

The works performed in the Separation Chemistry Group of the Chemistry Division of Argonne National Laboratory on the transport and separation properties of supported liquid membranes (SLM) are reviewed. The models and equations which describe the permeation through SLMs of metal species are described. These models have been tested with various carriers absorbed on flat-sheet and hollow-fiber SLMs by measuring the permeation of several metal species of hydrometallurgical and nuclear interest. An equation for the separation factor of metal species in SLM processes and examples of separations of metal ions are reported. The possibility of bypassing the single stage character of SLM separations by using multilayer composite SLMs, arranged in series, is also analyzed. Finally, the factors which control the stability of SLMs are briefly discussed.

INTRODUCTION

The possibility of utilizing thin layers of organic solutions of solvent extraction reagents, immobilized on microporous inert supports interposed between two aqueous solutions, for removing selectively metal ions from a mixture was first proposed more than 20 years ago (*1*). Such immobilized liquid layers, representing supported liquid membranes (SLM), have since then attracted the interest of a number of researchers. Their transport properties with respect to metal species present in aqueous solutions have been described in Refs. *2* to *6*. SLMs represent an attractive alternative to liquid–liquid extraction for the selective removal and concentration of metal

 0149-6395/84/1911-0857$3.50/0

ions from solutions, and some interesting papers have been published describing their possible application to the recovery of metals such as Cu, U, Cr, Co, and Ni (*7–11*).

The permeation of metal species through SLMs can be formally described as the simultaneous combination in a single stage of an extraction and a stripping operation, occurring in nonequilibrium conditions. A detailed knowledge of the liquid–liquid extraction equilibria and mass transfer kinetics is therefore required to understand and quantitatively describe the rate laws which control the permeation of metal species through SLMs and to exploit them for separative processes.

In view of our previous experience in liquid–liquid extraction equilibria and kinetics (*12*), we started in 1980 a research program in the field of SLMs having the following objectives:

To work out simple models which, in terms of a few and independently measurable variables, could describe quantitatively the permeation process of metal species through SLMs of low dielectric constant.
To apply the developed knowledge to the separation and recovery of metals of critical and strategic importance and to the decontamination of hazardous radioactive wastes.

SLMs appear particularly promising for these kind of processes in view of the following advantages over other traditional separation technologies:

Lower capital and operating cost
Low energy consumption
The possibility of using economically expensive, tailor-made extractant molecules
The possibility of achieving high separation factors
The possibility of concentrating the recovered species during the separation

In the present paper a short state-of-the-art review of the research activity (*13–24*) carried out in our laboratory during the last 4 years in the field of transport and separation of metal species through SLMs is presented.

COUPLED TRANSPORT THROUGH SUPPORTED LIQUID MEMBRANES

The mechanism of coupled transport through SLMs is schematically described in Fig. 1. The SLM consists of a solution, in a water-immiscible low dielectric constant organic diluent, of an extracting reagent—a metal

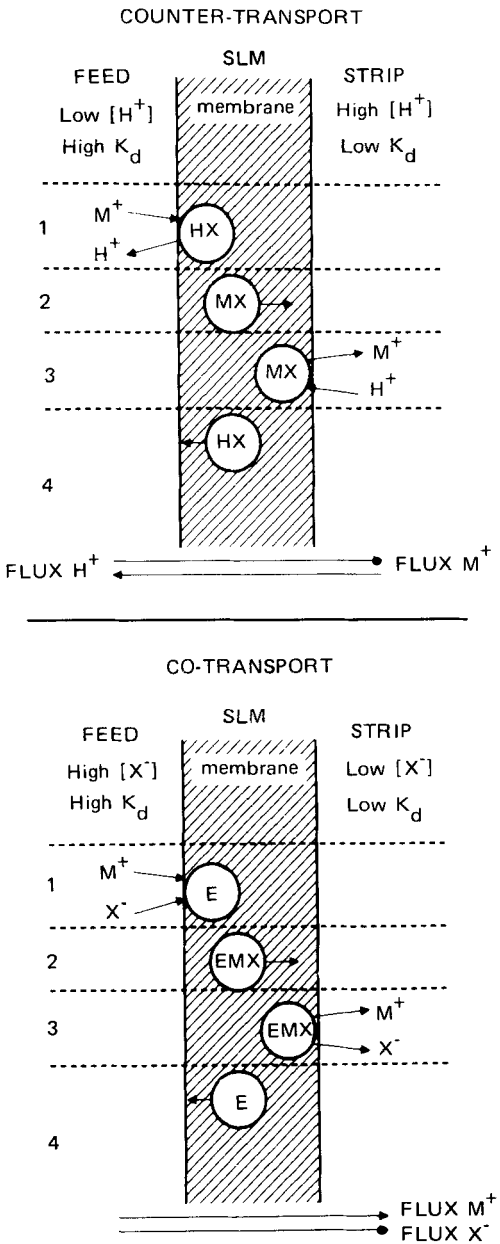

FIG. 1. Schematic description of coupled transport of a monovalent metal cation M^+ through a supported liquid membrane. HX and E represent the membrane carriers. X^- is an aqueous soluble counterion.

carrier in membrane terminology—absorbed on a microporous polymeric film having a thickness ranging from 25 to 50 μm. The polymeric film, which acts as solid support of the liquid membrane, is generally made of polypropylene, polysulfone, or other hydrophobic materials and has pore sizes ranging from 0.02 to 1 μm. The SLM is interposed between two aqueous solutions. The aqueous solution, initially containing all the metal ions which can permeate the SLM, is referred to as the feed solution. The distribution ratio between the organic phase absorbed in the membrane pores and the aqueous feed solution of the metal species permeating the SLM, K_d, is here high enough to favor metal extraction into the membrane phase. The aqueous solution present on the opposite side of the membrane, which is initially free from the permeable metal ions, is referred to as the strip solution. In this case the distribution ratio K_d is made as low as possible in order to favor complete back extraction of the metal species from the liquid membrane. If the metal carrier is an acidic extractant, HX, the difference in K_d between the feed and strip sides of the SLM is generally achieved by a pH gradient. In this case we deal with a counter-transport phenomenon (Fig. 1, upper part) and the chemical reaction which is responsible for the coupled transport can be schematized as

$$M^+ + \overline{HX}\ (\text{membrane}) \underset{\text{strip side}}{\overset{\text{feed side}}{\rightleftharpoons}} MX\ (\text{membrane}) + H^+ \qquad (1)$$

If the metal carrier is a neutral or a basic extractant (i.e., a long-chain alkylamine), E, the difference in K_d between feed and strip is generally obtained by a concentration gradient of the counterion, X^-, which is accompanying the metal cation into the membrane. In this case we deal with a co-transport phenomenon (Fig. 1, lower part) and the chemical reaction which is responsible for the coupled transport can be schematized as

$$M^+ + X^- + \bar{E}\ (\text{membrane}) \underset{\text{strip side}}{\overset{\text{feed side}}{\rightleftharpoons}} \overline{EMX}\ (\text{membrane}) \qquad (2)$$

pH and counterion concentration gradients are most often used as driving forces. However, any other expedient which assures a large chemical potential gradient between the two opposite sides of the membrane can be

used as long as coupled transport of metal ions and some other chemical species occurs through the SLM.

From this schematic description of coupled transport it follows that metal species can be transported across the membrane against their concentration gradient. This type of "uphill" transport will continue until all the metal species which can permeate the SLM have been transferred from the feed to the strip side, providing the driving force of the process is kept constant. This situation often occurs in practice when very dilute solutions of metal species are involved or when, in the case of more concentrated metal solutions, the concentration of the chemicals responsible for the driving force is continuously adjusted to keep it constant. It follows that in a SLM permeation process very high concentration factors can be obtained by using a volume of the strip solution which is much lower than that of the feed solutions. Moreover, by using carrier molecules, HX or E, which are very selective to given metal species, very clean separation processes can be performed. Since during the permeation the carrier acts as a shuttle, moving metal species from the feed to the strip solution and then diffusing back (being continuously regenerated during the process), very small amounts of carrier are used in SLM separations. As a consequence also, very expensive, highly selective, tailor-made carriers can be used economically. Other potential advantages of SLM separations over separations performed by traditional solvent extraction techniques are the lack of solvent entrainment phenomena (leading to high separation factors), the possibility of handling feed solutions containing suspended solids, the simplicity of the equipment involved, and the low energy consumption of the process. Moreover, with respect to separation processes performed with solid membranes, SLMs offer the additional advantage of higher fluxes since diffusion in liquids is much faster than in solids. The advantages offered by SLM separations are summarized in Table 1.

TABLE 1
Major Advantages of SLM Separations

High selectivities
Ions can be pumped "uphill"
Fluxes are higher than with solid membranes
Lower capital and operating cost
Expensive extractants can be utilized
High separation factors are achieved in a single stage
High feed/strip volume ratios

EQUATIONS DESCRIBING THE MEMBRANE TRANSPORT

The various steps which characterize the transport of metal species through SLMs can be described with the help of Fig. 1. *Step 1:* The metal species, after diffusing to the feed solution–SLM interface, react with the metal carrier. H^+ ions are simultaneously released into the feed solution (counter-transport, acidic carrier) or X^- ions accompany the metal ions into the membrane (co-transport, neutral or basic carriers). *Step 2:* The metal–carrier complex diffuses across the membrane because its concentration gradient is negative. *Step 3:* At the SLM–strip solution interface the metal–carrier complex releases metal ions into the aqueous phase. H^+ ions replace the M^+ ions into the membrane (counter-transport) or X^- ions are simultaneously released together with M^+ ions into the strip solution (co-transport). *Step 4:* The uncomplexed carrier diffuses back across the membrane.

When the distribution ratio at the membrane–aqueous strip interface is much lower than at the membrane–aqueous feed interface and the membrane phase polarity is low enough to make negligible the concentration of charged species with respect to that of uncharged ones, the steady-state overall membrane flux can be derived by applying Fick's diffusion law to the aqueous boundary layer present on the feed side of the membrane, to the membrane itself, and by expressing the interfacial flux in terms of the interfacial kinetics. If the concentration of the metal-containing species is much lower than that of the carrier and of the H^+ or X^- ions in the feed solution, their concentration gradients are practically constant and the three equations which describe the fluxes are

$$J_a = -D_a \frac{\partial [M^+]}{\partial x} \tag{3}$$

(diffusion through the aqueous boundary layer) where D_a is the aqueous diffusion coefficient of the metal-containing species,

$$J_b = K_1 [M^+]_i - K_{-1} [\bar{M}]_i \tag{4}$$

(interfacial flux) where K_1 and K_{-1} are the pseudo-first-order rate constants of the interfacial reactions described in Eq. (1) or (2); $[M^+]_i$ and $[\bar{M}]_i$ are the interfacial concentrations of the metal containing species at the feed solution–membrane interface on the aqueous and membrane side, respectively,

$$J_c = -D_0 \frac{\partial[\bar{M}]}{\partial x} \tag{5}$$

(membrane diffusion), where D_0 is the membrane diffusion coefficient of the metal-containing species $\bar{M}$. At the steady state $J_a = J_b = J_c$, and by further assuming linear concentration gradients, the following equation holds for the membrane flux, J, and the permeability coefficient P.

$$P = \frac{J}{C} = \frac{K_1}{K_1 \Delta_a + K_{-1} \Delta_0 + 1} \tag{6}$$

The meanings of d_a, d_0, Δ_a, and Δ_0 as well as a schematic description of the processes involved are shown in Fig. 2. C is the time-dependent bulk concentration of the metal species in the feed solution. By dividing the numerator and the denominator of Eq. (6) by K_{-1} and considering that

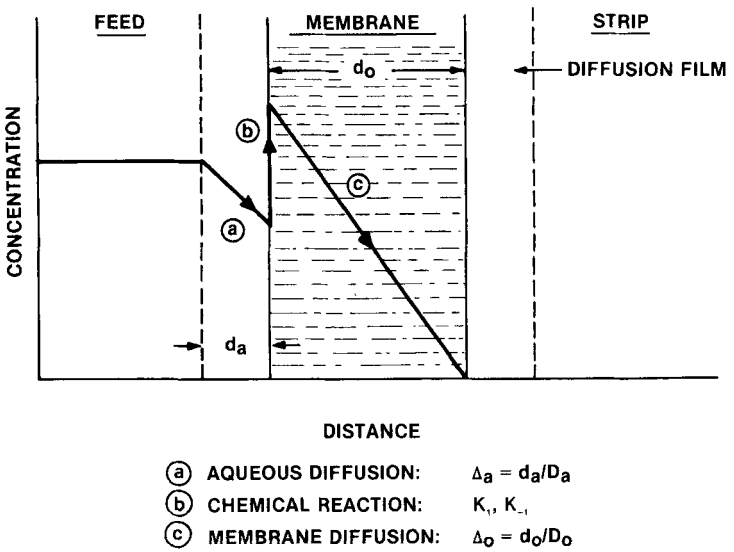

FIG. 2. Schematic description of the processes controlling the permeation rate through a SLM when the distribution ratio at the membrane–strip solution interface is much lower than at the membrane–feed solution interface.

$K_1/K_{-1} = [\overline{M}]/[M^+] = K_d$, when the interfacial chemical reactions are very fast (local equilibrium), Eq. (6) further simplifies to

$$P = \frac{J}{C} = \frac{K_d}{K_d\Delta_a + \Delta_0} \tag{7}$$

Since the relationship which correlates the membrane flux to C, to the aqueous feed volume V, and to the membrane area Q is

$$J = -\frac{dC}{dt}\frac{V}{Q} \tag{8}$$

the integrated form of the flux equation is

$$\ln\frac{C}{C_0} = -\frac{Q}{V}Pt \tag{9}$$

C_0 is the value of C at time zero. Equations (7) and (9) are very useful to predict the permeation behavior of SLMs when the feed solutions are relatively dilute in metal species. In this case the permeability coefficient is a time-independent parameter containing the chemical and diffusional parameters characteristic of each metal ion permeating a given SLM in contact with a given aqueous feed solution. Equation (7) indicates that the flux J varies with C. When the feed solutions contain metal ions at relatively high concentrations, and Reactions (1) or (2) are completely shifted to the right, K_d is not any longer independent of C. The highest value of $[\overline{M}]$ is $[\overline{HX}]/n$ (counter-transport) of $[\overline{E}]/n$ (co-transport) and the distribution ratio $K_d = [\overline{M}]/C$ becomes inversely dependent on C. n is the number of carrier molecules per metal ion in the metal–carrier complex and $[\overline{HX}]$ and $[\overline{E}]$ are the total carrier concentrations in the SLM. In this situation, for counter-transport, Eq. (7) becomes

$$\frac{J}{C} = \frac{([\overline{HX}]/nC)}{([\overline{HX}]/nC)\Delta_a + \Delta_0} \tag{10}$$

and for sufficiently large values of C

$$J = \frac{[\overline{HX}]}{n\Delta_0} \tag{11}$$

An identical equation holds for co-transport by replacing $[\overline{HX}]$ with $[\bar{E}]$. In order for Eq. (11) to hold, the further assumption that the membrane counter-diffusion of the carrier is a very fast process with respect to the diffusion of the metal–carrier complex must be introduced. Equation (11) can be integrated to

$$C = C_0 - \frac{[\overline{HX}]}{n\Delta_0} \frac{Q}{V} t \tag{12}$$

Equation (12) shows that the metal concentration in the feed solution decreases linearly with time. Therefore, the time-independent flux is a more useful parameter to describe the permeation of metal species through SLMs. Obviously, during the permeation of the metal species, starting with relatively high metal concentrations, there is a transition region where the decrease of concentration with time is expressed neither by Eq. (12) nor by

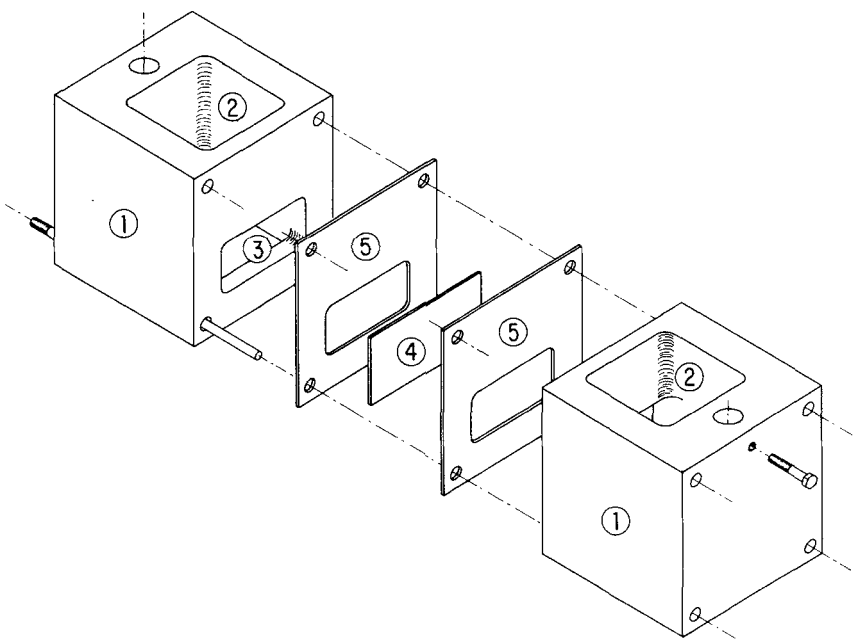

FIG. 3. Exploded view of an apparatus used to perform membrane permeation experiments with flat-sheet SLMs. (1) Plexiglass block, (2) chambers containing the aqueous feed and strip solutions, (3) opening facing the membrane, (4) SLM, and (5) Teflon gaskets.

Eq. (9). In this region the flux equation cannot be analytically integrated and a numerical solution for the integrated flux equation, containing a concentration-dependent P, has to be obtained. This situation has been described in detail in Refs. *18* and *20*.

EXPERIMENTAL VERIFICATION OF THE PERMEABILITY EQUATIONS

We have verified the validity of the equations reported in the previous section by studying the permeation behavior of several metal species using SLMs containing different metal carriers. The SLMs have been studied in two different shapes, i.e., as flat-sheet and hollow-fiber membranes. Figure 3 shows a typical experimental apparatus used by us for studying the

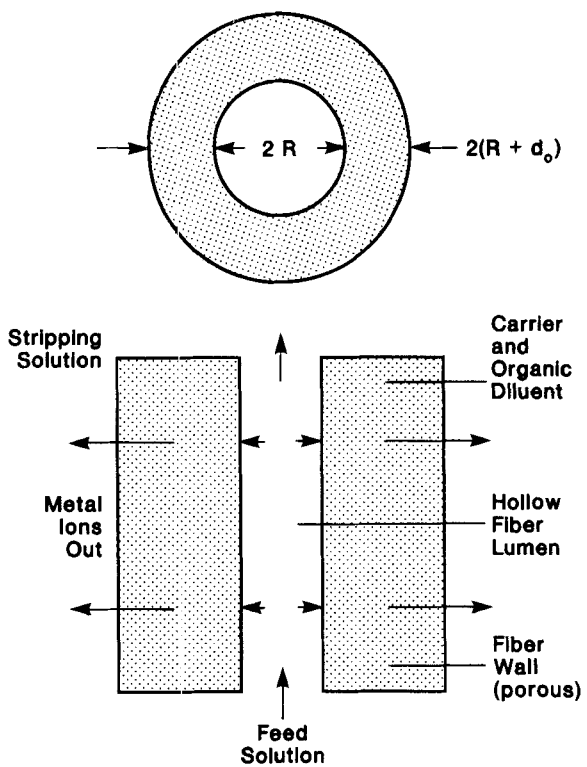

FIG. 4. Schematic representation of the axial and cross section of a hollow-fiber SLM of radius R and wall thickness d_0.

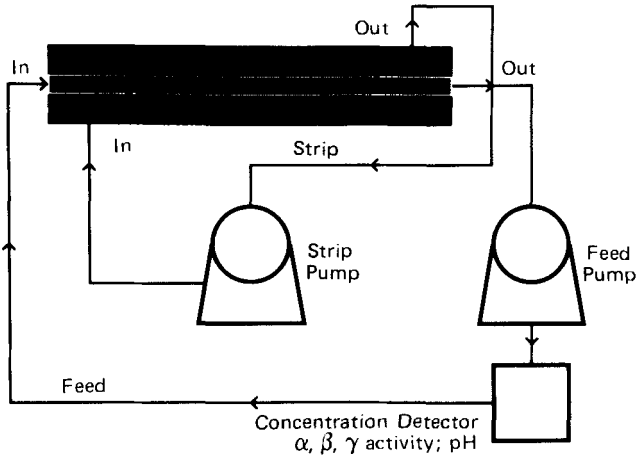

FIG. 5. Single hollow-fiber module used in a recycling mode.

permeation of metal species through flat-sheet SLMs (*17*). The concentration variations of the metal species with time were followed by on-line analytical techniques (radiochemical flow-cells, amperometry, potentiometry, oscillopolargraphy) or by intermittent sampling of the aqueous solutions followed by chemical or radiochemical analysis. In this way various sets of primary data, in the form C vs time, were obtained as functions of the composition of the aqueous solutions and of the SLM, the membrane area, the aqueous volumes, and the stirring speed of the feed and strip solutions. In the case of hollow-fiber SLMs, the organic solution of the carrier was absorbed in the microporous walls of polymeric supports shaped as tiny hollow tubes. A schematic representation of the cross and axial sections of a hollow-fiber SLM is shown in Fig. 4. The feed solution circulated through the lumen and the strip solution on the shell side of the hollow fibers. A typical experimental arrangement used by us is shown in Fig. 5. In most experiments single hollow-fiber SLM modules operated in a recycling mode were used. Both the feed and strip solutions always flowed in a laminar regime although the feed residence time in the fibers was always much shorter than the half-time of the permeation process. When these conditions hold, the hollow-fiber SLM of radius R and length L behaves as a flat-sheet SLM of area $2\pi RL$ in contact with an aqueous solution of volume equal to the total volume of the recirculating solution.

The validity and the meaning of the equations reported in the previous section can be illustrated using as an example the SLM system shown in Fig. 6 taken from Ref. *18*. The chemical reaction which is here responsible for the co-transport of Am^{3+} and NO_3^- ions through the SLM is

CMPO = n-octyl(phenyl)-N,N-diisobutyl-carbamoylmethyl phosphine oxide

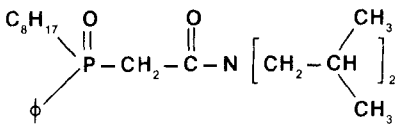

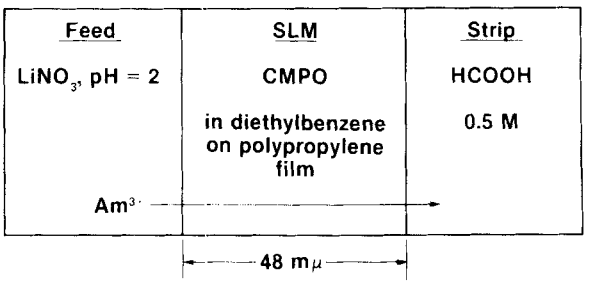

FIG. 6. Schematic description of the SLM system used for the transport study of Am^{3+} with the neutral bifunctional carrier CMPO.

$$Am^{3+} + 3NO_3^- + 3\overline{CMPO}\,(\text{membrane}) \underset{\text{strip side}}{\overset{\textit{feed side}}{\rightleftharpoons}} \overline{Am(NO_3)_3 \cdot 3CMPO}\,(\text{membrane}) \qquad (13)$$

An example of primary C vs time data is reported in Fig. 7 for the two different initial metal concentrations: $C_0 = 10^{-6}$ M (Curve A) and $C_0 = 10^{-2}$ M (Curve B). For $C_0 = 10^{-2}$ M, Sm^{3+} (spiked with ^{241}Am) was used as a stand-in for Am^{3+}. When $C \leq 10^{-3}$ M the data points fall on a straight line of slope $-(Q/V)P$ which allows one to calculate the permeability coefficient of the SLM. These results confirm the validity of Eq. (9) to describe the concentration vs time data. On the other hand, the data points of Curve B, describing the first 18×10^3 s of the experiment, yield a straight line when plotted as C vs time. In this region the membrane permeability is entirely controlled by membrane diffusion, and Eq. (12) describes the concentration variation with time. In Fig. 8 the linear dependency of $[Am^{3+}]$ vs time is shown for two different concentrations of CMPO in the SLM. The straight lines are in agreement with the prediction of the theory, and their slopes increase when the carrier concentration increases. The validity of Eq. (7) to

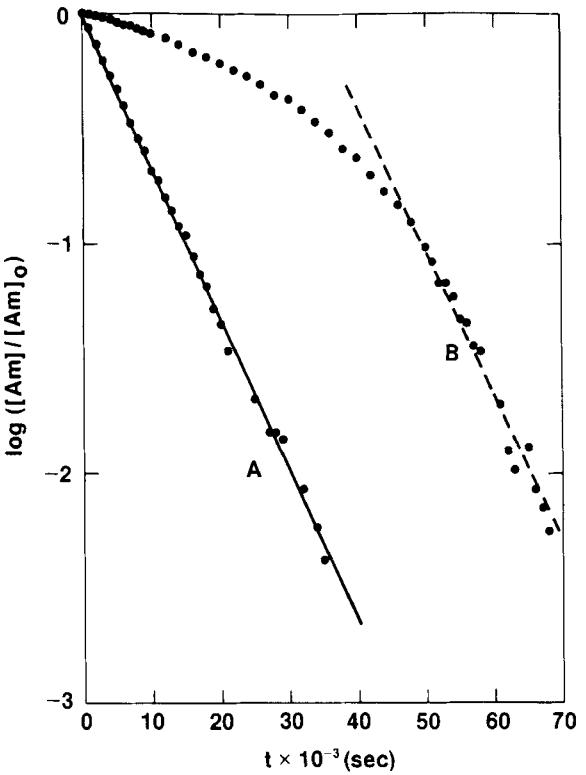

FIG. 7. Semilogarithmic plot of the Am^{3+} concentration vs time (s), through a [CMPO] = 0.1 *M* SLM. Feed: $[LiNO_3] = 2$ *M*, pH = 2. Strip: [HCOOH] = 0.5 *M*. Stirring = 250 rpm. A: ^{241}Am at tracer levels. B: $^{241}Am + [Sm^{3+}]_0 = 0.01$ *M*.

describe the permeation of metal species through SLMs is shown in Figs. 9 to 11, where the metal is present at tracer level concentrations. The data of Fig. 9(A) show that when the stirring speed of the aqueous solutions is greater than 100 rpm, P becomes independent of it. This independence indicates that a constant and minimum value of the thickness of the aqueous boundary layer, d_a, is reached. The data of Fig. 9(B) confirm the expected independence of P from the membrane area and aqueous volume, indicating that aqueous bulk chemical processes do not control the SLM permeability. Figures 10 and 11 show the dependence of P on the aqueous nitrate activity in the feed solution, a, at constant membrane composition, and on the membrane carrier concentration $[\bar{E}]$, at constant aqueous feed composition, respectively. The shape of the curves described by the data points and the agreement between the experimental points and the solid lines, calculated

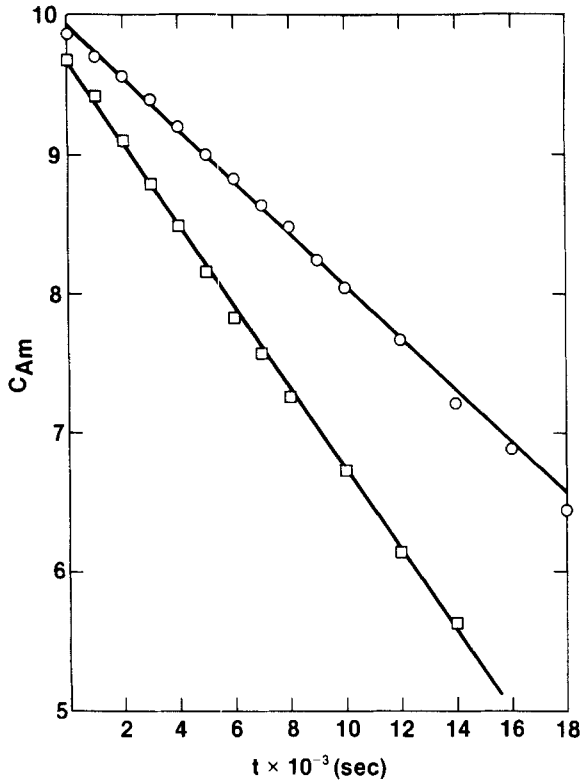

FIG. 8. Linear plot of the Am^{3+} concentration in the feed solution vs time (s). SLM: (○) [CMPO] = 0.1 *M*, (□) [CMPO] = 0.5 *M*.

through Eq. (7), indicate that the model used to derive the permeability equation gives a suitable description of the rate-controlling phenomena. The first portions of the log P vs log a and of the log P vs log $[\bar{E}]$ plots, yielding straight lines with a positive slope, have the same slopes as the corresponding log K_d vs log a and log K_d vs log $[\bar{E}]$ plots. In these regions the membrane permeability coefficient can be described only by the term $P = K_d/\Delta_0$, and the permeation process is entirely controlled by membrane diffusion. When the log P vs log a and log P vs log $[\bar{E}]$ curves become independent of the concentration terms (plateau region), the SLM permeability coefficient can be only described by the term $P = \Delta_a^{-1}$ and the permeation process is fully controlled by the diffusion of the metal species through the aqueous boundary layers. The position of this type of P curves on the x–y plane is a function of the chemistry of each SLM system (through K_d, D_a, and D_0), of

the aqueous stirring rate (through d_a), and of the membrane thickness (through d_0). From the slope of the straight line portion of the P curves and their plateau values, the two diffusional parameters Δ_a and Δ_0 can be calculated. If the diffusion coefficient of the metal species in the aqueous feed, D_a, and the membrane thickness, d_0, are known, the thickness of the aqueous boundary layer, d_a, and the diffusion coefficient of the carrier–metal complex in the SLM, D_0, can also be obtained.

In the case of hollow-fiber SLMs operated in a recycling mode, the same equations, (7) to (12), describe the permeation process, providing the flow rate through the SLM lumen is high enough. Figure 12 shows the dependence of the permeability coefficient on the linear flow velocity of the feed stream circulating in the fiber lumen. The data refer to the same liquid membrane system described in Fig. 6, except that a hollow-fiber microporous polypropylene support was used and the diluent dissolving CMPO was the mixture 67% decalin + 33% diisopropylbenzene. The data points indicate that by increasing the feed flow rate, a constant value of P is reached at

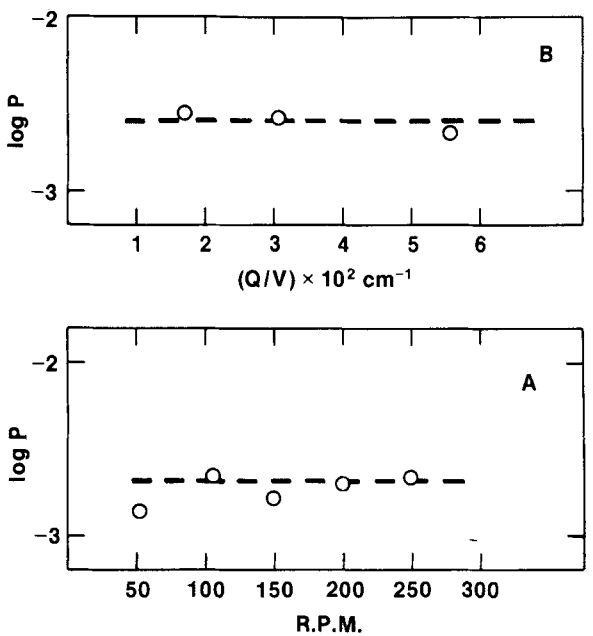

FIG. 9. A: Membrane permeability coefficient P (cm/s) of Am^{3+} tracer vs stirring speed of aqueous feed and strip solutions in rpm. B: Membrane permeability coefficient P (cm/s) of Am^{3+} tracer vs (membrane area/aqueous feed volume), Q/V. Feed and strip as in Fig. 7A. SLM: [CMPO] = 0.5 M.

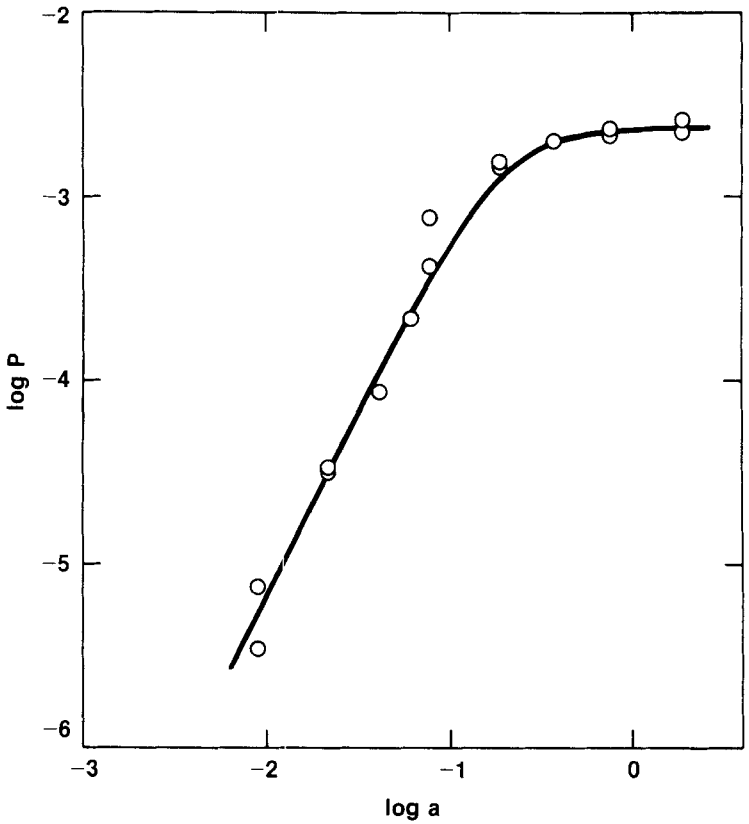

FIG. 10. Am^{3+} permeability coefficient P (cm/s) vs aqueous feed $LiNO_3$ molar activity, a. SLM: [CMPO] = 0.5 M. The solid line was calculated from Eq. (7).

moderate values of the feed linear flow velocity. This constant value can be interpreted as occurring when a minimum and constant thickness of the aqueous boundary layer is reached inside the fiber lumen.

Table 2 summarizes the SLM systems which we have so far investigated in detail in our laboratory. All systems have confirmed the validity of the developed model, and the equations which follow from it, to describe quantitatively the permeation of the metal species through the SLMs. The data indicate that higher membrane diffusion coefficients are obtained with aromatic diluents. However, since aromatic diluents slowly chemically attack the microporous polypropylene support, aliphatic solvents are preferable. In all the studied systems, the K_d's at the SLM–strip solution interface were much lower than at the SLM–feed solution interface.

TABLE 2
List of SLM Systems Investigated in Detail in Our Laboratory[a]

Ion	Feed	Strip	Carrier–diluent[b]	D_0 (cm^2/s)
Eu^{3+}	HCl	HCl	HDEHP–dodecane	2×10^{-7}
Cu^{2+}	HCl	HCl	Oxime–toluene	2.2×10^{-6}
Am^{3+}	$LiNO_3$	HCOOH	OφD[IB]CMPO–diethylbenzene	2.4×10^{-6}
Zn^{2+}, Cd^{2+}	HCl	CH_3COONH_4	TLA–triethylbenzene	3.2×10^{-6}
Co^{2+}, Ni^{2+}	CH_3COOK	HCl	Dialkylphosphinic acid Decalin–DIIPB	3×10^{-7}
	$NaNO_3$	NaOH	TLA–dodecane	4.4×10^{-7}
	$NaNO_3$	NaOH	TLA–diethylbenzene	6.5×10^{-6}
	$NaNO_3$	NaOH	Primene JMT–diethylbenzene	6.5×10^{-6}
H^+	$NaNO_3$	NaOH	TOPO–diethylbenzene	—
	$NaNO_3$	NaOH	OφD[IB]CMPO–diethylbenzene	—
	$NaNO_3$	NaOH	DHDECMPO–diethylbenzene	—

[a] Support: Microporous polypropylene.
[b] HDEHP = di(2-ethylhexyl)phosphoric acid (*14*).
Oxime = 2-hydroxy-5-tert-octylacetophenone oxime (*15*).
OφD[IB]CMPO = *n*-octyl(phenyl)-*N,N*-diisobutylcarbamoylmethylphosphine oxide (*18*).
TLA = tri-dodecylamine (*19, 20*).
Dialkylphosphinic acid = di(2,4,4'-trimethylpentyl)phosphinic acid (*25*).
Primene JMT = *t*-$C_{18}H_{37}NH_2$ to *t*-$C_{22}H_{45}NH_2$ (*20*).
TOPO = tri-*n*-octylphosphine oxide (*19*).
DHDECMPO = dihexyl-*N,N*-diethylcarbamoylmethylphospine oxide (*19*).
DIIPB = diisopropylbenzene, decalin = decahydronaphthalene.

Consequently, the permeation rates were always independent of the stirring rate (flat-sheet SLMs) or the flow rate (hollow-fiber SLMs) of the strip solutions.

SEPARATION OF METAL SPECIES

The possibility of separating two or more metal species by SLMs exists whenever the species are characterized by sufficiently different values of the permeability coefficients. By introducing a membrane separation factor, α, defined as the ratio of the permeability coefficients of the metal species we want to separate, it follows from Eq. (7) that

$$\alpha = \frac{P_1}{P_2} = \frac{K_{d1}}{K_{d2}} \left(\frac{K_{d2}\Delta_a + \Delta_0}{K_{d1}\Delta_a + \Delta_0} \right) \tag{14}$$

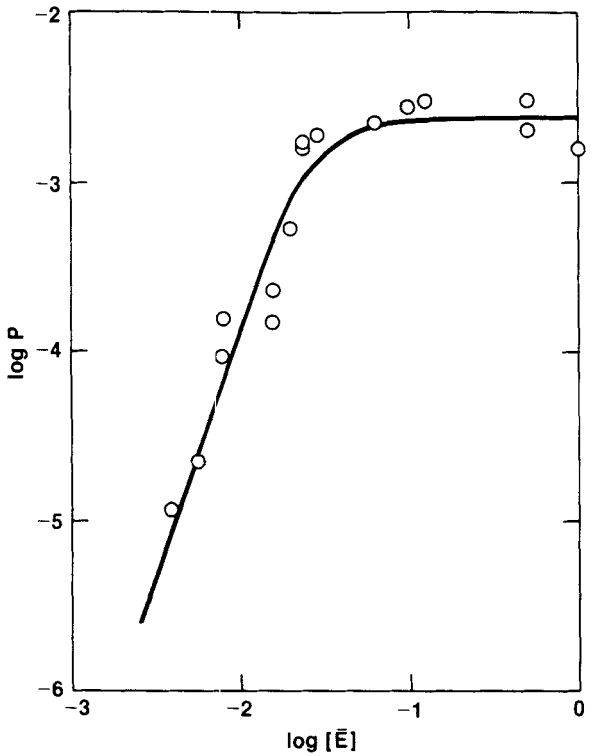

FIG. 11. Am^{3+} permeability coefficient P (cm/s) vs CMPO molar concentration in the membrane phase [Ē]. Feed and strip as in Fig. 7A. The solid line was calculated from Eq. (7).

The subscripts 1 and 2 refer to the two metal species M_1 and M_2. Since the aqueous diffusion coefficients of most metal species and most metal–carrier complexes have very similar values in similar solution environments, the diffusional parameters Δ_a and Δ_0 are practically equal for two simultaneously diffusing metal species and represent nonselective terms which reduce the selectivity of the SLM. When the term $K_d\Delta_a$ is much smaller than Δ_0 in both the numerator and the denominator of Eq. (14), the separation factor reaches its maximum value, equal to

$$\alpha_{\max} = K_{d1}/K_{d2} \tag{15}$$

Equation (15) indicates that the highest separation factor which can be obtained with a SLM is equal to the separation factor obtained in a solvent

extraction process which utilizes the same liquid membrane as an extracting phase. This situation occurs either when very thick SLMs are used and/or when the thickness of the aqueous boundary layer becomes extremely small. The latter situation is of course more desirable than the former one from a practical point of view since it does not imply a slowdown of the membrane permeation rate of the metal species. From Eq. (14) it also follows that the SLM completely loses its selectivity, i.e., $\alpha_{\min} = 1$, when for both metal species $K_d\Delta_a \gg \Delta_0$. This situation arises either when poorly stirred feed solutions are used or the K_d values of both metal species are extremely high. However, in most practical cases dealing with the separation and recovery of metal species from dilute solutions, intermediate situations occur. In practice, since it is not possible to minimize beyond a given value the thickness of the aqueous boundary layers, d_a, and the membrane thickness, d_0, the membrane selectivity is maximized by choosing a selective carrier and adjusting its concentration and the composition of the feed solution in such a way as to approach as close as possible the condition $K_{d1} \gg 1$ and

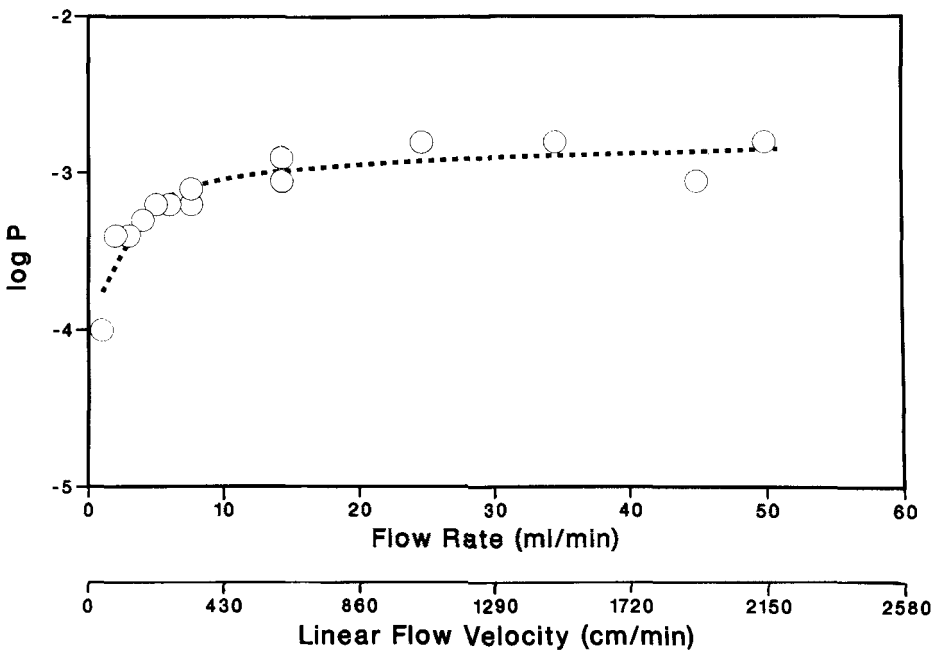

FIG. 12. Am^{3+} permeability coefficient through a single hollow-fiber module P (cm/s) vs flow rate (mL/min) or linear flow velocity (cm/min) of the feed solution. Feed and strip solutions as in Fig. 7A. SLM: [CMPO] = 0.1 M in 67% decalin + 33% diisopropyl-benzene supported on an Accurel polypropylene hollow fiber.

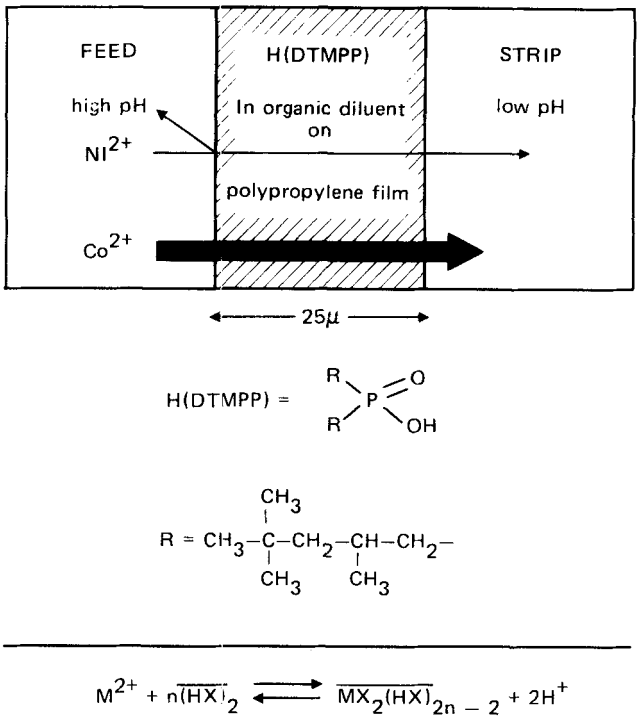

FIG. 13. Schematic description of the SLM system used to separate Co^{2+} from Ni^{2+}. Organic diluent: 67% decalin + 33% diisopropylbenzene. $M^{2+} = Co^{2+}$ or Ni^{2+}.

$K_{d2} \ll 1$. When this condition holds, since for most SLMs d_0 ranges from 25 to 50 μm and for most well-stirred aqueous solutions d_a ranges from 15 to 40μm, it follows from Eq. (7) that $P_1 = \Delta_a^{-1}$, $P_2 = K_{d2}\Delta_0^{-1}$, and $\alpha = \Delta_0/(\Delta_a K_{d2})$. By considering that (a) d_a and d_0 have approximately the same value and (b) for a typical aliphatic diluent which is compatible with the support $D_a/D_0 \sim 10$, the separation factor is then only related to the distribution ratio of the least extractable metal M_2 through the equation

$$\alpha \sim 10/K_{d2} \tag{16}$$

Equation (16) is an approximate relationship which can sometimes be used as a rule of thumb to evaluate the magnitude of the separation factor holding in a SLM separation process performed under typical operational conditions with a selective carrier. Since K_d always increases with the concentration of the extractant which is not bound to the metal, it follows from Eq. (16) that

high separation factors are favored by low concentrations of the unbound carrier as long as K_{d1} can be maintained sufficiently high.

Very high separation factors can also be obtained when the carrier is loaded with the more extractable metal. As an example of this effect we may consider the Co–Ni separation performed with the SLM system schematically shown in Fig. 13 and described at length in Ref. *25*. Here the liquid membrane used was a solution of di(2,4,4′-trimethylpentyl)phosphinic acid, H(DTMPP), in the 67% decalin + 33% diisopropylbenzene diluent mixture and the feed solution contained a 1 *M* acetate buffer at pH = 6. The equation for the SLM Co–Ni separation factor is (*25*)

$$\alpha = \frac{6 \times 10^2}{[\overline{HX}]^{0.6}} \frac{1.4 \times 10^3 [\overline{HX}]^2 + 1.1 \times 10^4}{2.2 \times 10^5 [\overline{HX}]^{1.4} + 1.1 \times 10^4} \qquad (17)$$

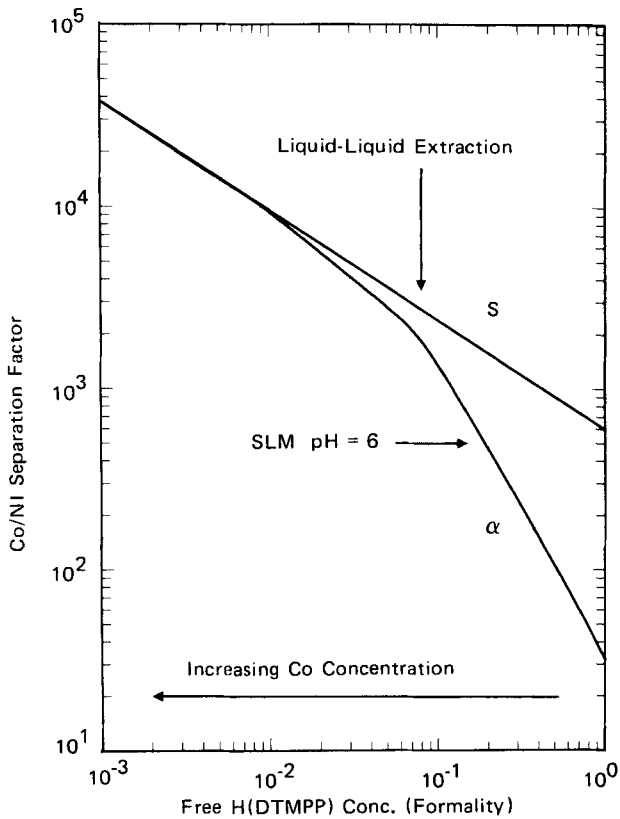

FIG. 14. SLM separation factor (α) and liquid–liquid extraction separation factor (S) for Co/Ni vs formal concentration of the unbound carrier H(DTMPP).

where the term

$$\frac{6 \times 10^2}{[\overline{HX}]^{0.6}} = \frac{K_d(\mathrm{Co})}{K_d(\mathrm{Ni})}$$

represents the separation factor, S, obtainable in a liquid–liquid extraction process under similar experimental conditions. $[\overline{HX}]$ is the formal concentration of the unbound carrier in the SLM. The variations of S and α with the concentration of the unbound H(DTMPP) is shown in Fig. 14. From these curves it can be predicted that very clean Co–Ni separations can be obtained

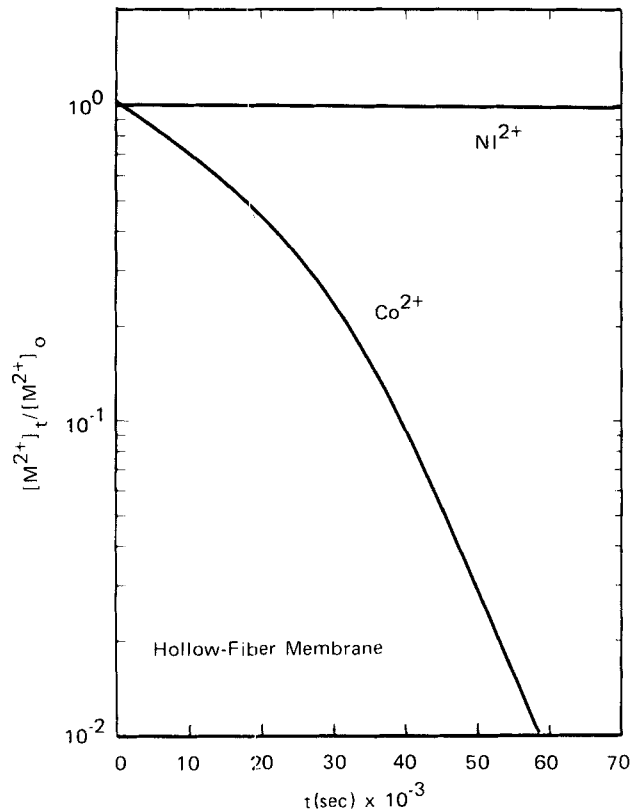

FIG. 15. Semilogarithmic plot of the cobalt and nickel concentrations, $[M^{2+}]_t/[M^{2+}]_0$, vs time (s) for the permeation through a single hollow-fiber SLM. Feed: $[CH_3COOK] + [CH_3COOK] = 1.0$ *M*, pH = 6, $[Co^{2+}]_0 = [Ni^{2+}]_0 = 0.1$ *M*. SLM: [H(DTMPP)] = 0.5 *M* in 67% decalin + 33% diisopropylbenzene. Strip: [HCl] = 1 *M*. Feed flow rate: 20 cm^3/min. $[M^{2+}]_t$ and $[M^{2+}]_0$ are the metal concentrations at time *t* and time zero, respectively.

TABLE 3
Molar Concentration of Ions in a Synthetic Acidic Nuclear Waste Solution

H^+	1.0
Al^{3+}	0.78
Fe^{3+}	0.16
Cr^{3+}	0.015
Ni^{2+}	0.007
Na^+	0.21
SO_4^{2-}	0.33
F^-	0.14
$NO_3^- + NO_2^-$	Balance of anions ~3
Actinides (U, Pu, Am, Cm)	$\sim 5 \times 10^{-4}$

by decreasing the concentration of the free carrier by increasing the carrier loading with cobalt. The experimental results obtained by using a hollow-fiber SLM, shown in Fig. 15, confirm this prediction. In the region where the total cobalt recovery is kept below 70%, the separation factor is very high ($>10^4$) and very pure cobalt (<0.1% Ni) can be recovered. By increasing the cobalt recovery to 90% or to 99%, the amount of Ni accompanying the cobalt increases to 0.4 and 1%, respectively. The decrease of selectivity of the Co–Ni separation is the result of the higher concentration of unbound H(DTMPP) in the liquid membrane.

When the objective of the SLM separation is to purify a feed solution from one or more metal species, which act as contaminants, the requirements on the separation factors are less stringent and the major concern is shifted from the recovery of high purity metals to the complete removal of the

TABLE 4
Molar Concentration of Fission Products in a Synthetic Acidic Nuclear Waste Solution

Ge	3×10^{-7}	In	0.5×10^{-6}
As	0.5×10^{-7}	Sn	2×10^{-5}
Se	0.25×10^{-4}	Sb	0.45×10^{-5}
Br	0.8×10^{-5}	I	1×10^{-4}
Rb	2×10^{-4}	Cs	0.8×10^{-3}
Sr	0.4×10^{-3}	Ba	0.6×10^{-3}
Y	2.5×10^{-4}	La	0.4×10^{-3}
Zr	1.8×10^{-3}	Ce	0.8×10^{-3}
Mo	1.6×10^{-3}	Pr	0.36×10^{-3}
Te	0.35×10^{-3}	Nd	1.25×10^{-3}
Ru	1×10^{-3}	Pm	0.85×10^{-5}
Rh	1.7×10^{-4}	Sm	0.25×10^{-3}
Pd	0.8×10^{-3}	Eu	0.5×10^{-4}
Ag	2.5×10^{-5}	Gd	0.35×10^{-4}
Cd	0.3×10^{-4}	Tb	0.55×10^{-6}

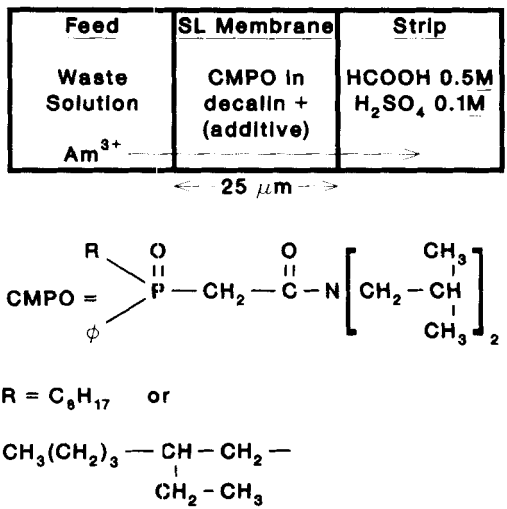

FIG. 16. Schematic description of the SLM system used to remove Am^{3+} and other actinides from the synthetic liquid waste whose composition is reported in Tables 3 and 4.

contaminating metal species. The removal of the long-living and highly radiotoxic transuranium elements from the liquid nuclear wastes produced during the processing of nuclear fuel represents such a case. A typical composition of a synthetic acidic nuclear waste produced in a Purex reprocessing plant is shown in Tables 3 and 4. A few actinides have to be removed from a complex mixture, containing about 40 different metal species, to the point that the waste can be successively treated for above ground storage without representing a potential health hazard. In this case neutral bifunctional extractants, such as those studied by Horwitz in Refs. *26* and *27*, can be used as carriers in a SLM to remove the actinides from the acidic waste solution. The SLM system and the bifunctional carrier which have been proposed for such a separation are schematically shown in Fig. 16. The additive is tributylphosphate, TBP, which is required to avoid third-phase formation. The chemistry of this system and its application to the decontamination of liquid nuclear wastes by solvent extraction has been thoroughly investigated in a series of papers by Horwitz and co-workers (*26, 27*). The chemical reactions which are responsible for the co-transport of Am^{3+} and HNO_3 through the SLM are shown in Fig. 17. The other actinides as well as the trivalent lanthanides behave very similarly to Am^{3+} and are simultaneously transported across the SLM (*24*). The same holds for Tc. Small amounts of the noble metals (Rh, Ru, and Pd), Fe, Zr, Mo, and Nb can also cross the SLM, although the addition of oxalate anions greatly

$$Am^{3+} + 3NO_3^- + \overline{3E(HNO_3)_m} \rightleftharpoons \overline{Am(NO_3)_3 \bullet E_3(HNO_3)_n} + (3m-n)HNO_3$$

$$HNO_3 + \overline{TBP} \rightleftharpoons \overline{TBP \bullet HNO_3}$$

$$E = CMPO$$

FIG. 17. Chemical reactions which are responsible for the co-transport of Am^{3+} and HNO_3 through the SLM of Fig. 16. From Horwitz et al. (*27*).

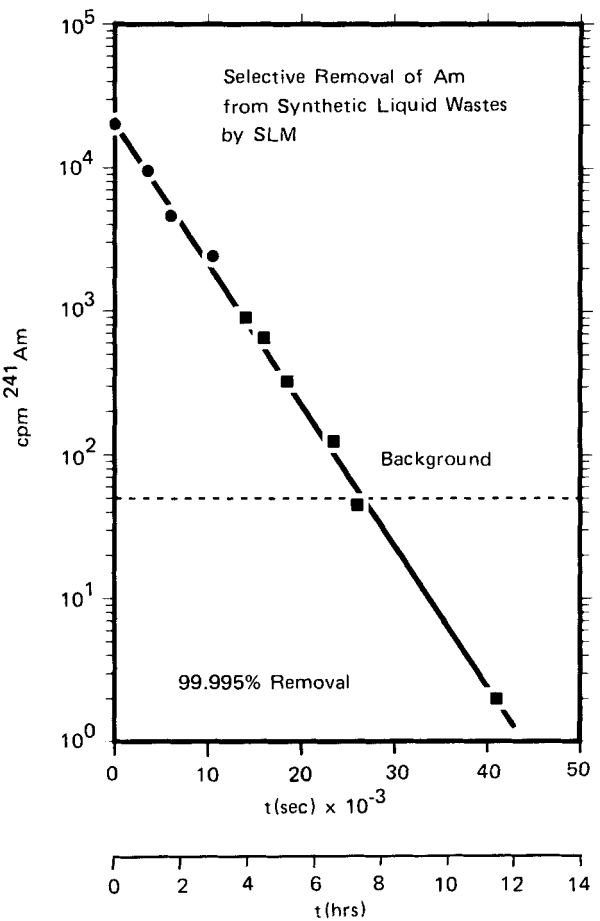

FIG. 18. Concentration (gamma counts per minute) vs time (s) plot for the transport of Am^{3+} through the SLM of Fig. 16.

reduces the permeability of these latter four metals (*26, 27*). Nevertheless, since in this case the objective of the SLM separation is the decontamination of the liquid waste from the actinides, and not their recovery in a very pure form, SLMs can still be considered as a possible separation technology, as long as the activity of the wastes is low enough not to damage the polypropylene support of the liquid membrane. A typical concentration vs time curve for the removal of Am^{3+} from a synthetic nuclear waste solution having the composition reported in Tables 3 and 4 is shown in Fig. 18. The data indicate that it is possible to achieve a good decontamination from Am^{3+}. Similar curves are also obtained with the other actinides (*24*). Since the metals are here present at low concentration, straight lines are always observed and the time-independent permeability coefficient of the metal species is the most suitable parameter for describing the SLM permeation process.

MULTISTAGE SEPARATIONS BY COMPOSITE SLMs

The separation processes we have discussed so far are based on the use of a single SLM and are therefore single stage. Since the composition of the strip solution must promote the back extraction of the metal species which have entered the SLM from the feed side (Solution A), it follows that if a second membrane having the same chemical nature as the first one (SLM(A)) is used in series with the first one, no further permeation can take place. This situation is schematically shown in Fig. 19. Therefore, if the permeability coefficients of the metal species to be separated by the SLM are

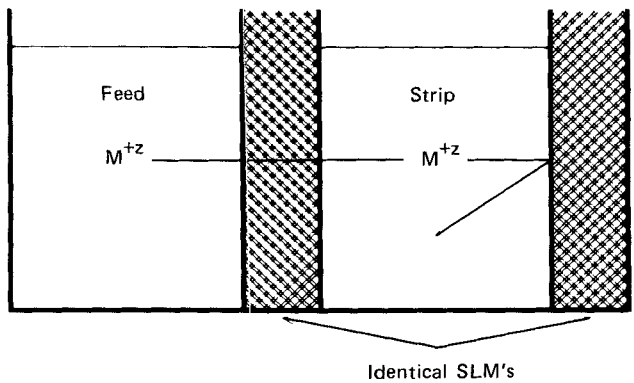

FIG. 19. Schematic description of the single stage character of SLM separations of metal ions in solution. M^{+z} cannot permeate the SLM from the strip solution.

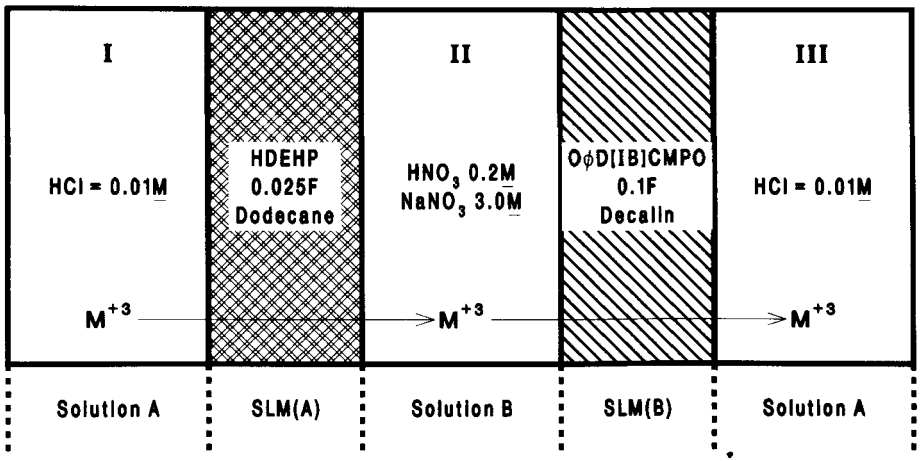

FIG. 20. Composite SLM system, containing an acidic (HDEHP) and a neutral (OφD[IB]CMPO) SLM, used to study the Eu^{3+}-Am^{3+} separation.

not very different, it is not possible to produce metal species in high purity because of the single-stage character of the process. In practice there are many cases where separations of metal ions having very similar chemical properties, and consequently very similar permeability coefficients, are required. In Refs. *22, 23*, and *28* we have described the possibility of bypassing the single-stage character of SLM separations of metal ions in solution by using composite SLMs. A composite SLM consists of a series of two complementary SLMs—SLM(A) and SLM(B)—with an aqueous solution of suitable composition (Solution B) sandwiched between them. The second membrane, SLM(B), is chosen in such a way that the intermediate aqueous Solution B, which promotes the stripping of the metal species from SLM(A), can also promote their extraction into SLM(B). Moreover, Solution A, which promotes the extraction of the metal species into SLM(A), also promotes their stripping from SLM(B). In this way the system "SLM(A)–Solution B–SLM(B)" can be viewed as a composite SLM, and as long as the overall permeabilities of the metal ions through the system "Solution A–SLM(A)–Solution B–SLM(B)–Solution A" show some difference, complete separations can be achieved by arranging a sufficiently large number of composite SLMs in series, each one separated by aqeuous compartments containing Solution A. An example of such a composite system is shown in Fig. 20. This composite SLM system can be efficiently used to separate ions of similar behavior such as Eu^{3+} and Am^{3+}. Both Eu^{3+} and Am^{3+} are extracted into the HDEHP and OφD[IB]CMPO membranes from $[HCl] = 0.01\ M$ and $[HNO_3] = 0.2\ M + [NaNO_3] = 3.0\ M$, respec-

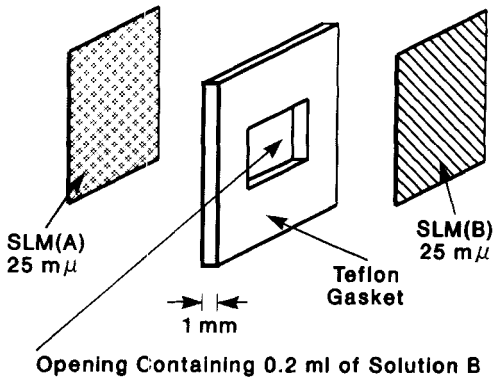

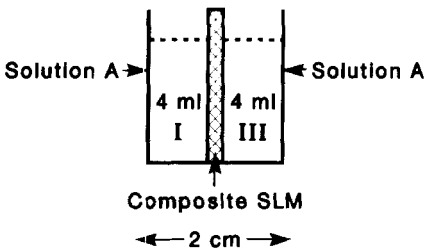

FIG. 21. Compact arrangement of the composite SLM of Fig. 20.

tively, while $[HNO_3] = 0.2\ M + [NaNO_3] = 3.0\ M$ and $[HCl] = 0.01\ M$ can completely strip the same ions from the HDEHP and OϕD[IB]CMPO membranes, respectively. Since the extraction K_d's of the two ions are different, the overall permeation rates of Eu^{3+} and Am^{3+} from Solution A, in Compartment I, to Solution A, in Compartment III, are different. When the concentrations of the permeating ions are much lower than those of all the other chemical species which contribute to the concentration gradients responsible for the driving force of the process, the composition of the various aqueous solutions stays practically constant with time, except for the variations in concentration of the permeating metal species. In this case the aqueous compartment containing Solution B can be reduced to a thin slab, sandwiched between the two SLMs, as schematically indicated in Fig. 21. In this way the composite SLM can be made very thin and many stages can be arranged in a limited space. Moreover, now the composite SLM behaves as a single membrane and the composite SLM permeability coefficient equals the permeability coefficient of the first membrane. For Eu^{3+} and Am^{3+} in the

experimental conditions of Ref. *23* these P values are equal to 2.3×10^{-3} and 4.5×10^{-4} cm/s, respectively. The results of a permeation experiment of Am^{3+} and Eu^{3+} through a single composite SLM are shown in Fig. 22. The ordinate scale represents the decrease in concentration in Compartment I in terms of the concentration increase in Compartment III. The straight lines allow one to evaluate the extent of Eu^{3+}/Am^{3+} separation which can be obtained in a single-stage process. If, for example, 90% of the initial Eu^{3+} is recovered, this will be accompanied by about 40% of the initial Am^{3+}. Therefore, no clean separation between the two cations can be obtained in a single stage because of the close values of $P(Eu^{3+})$ and $P(Am^{3+})$. Nevertheless, far better separations can be obtained if the single stage is repeated several times as shown in Fig. 23. For a series of i compartments containing identical volumes V of Solution A, separated by $i - 1$ identical composite

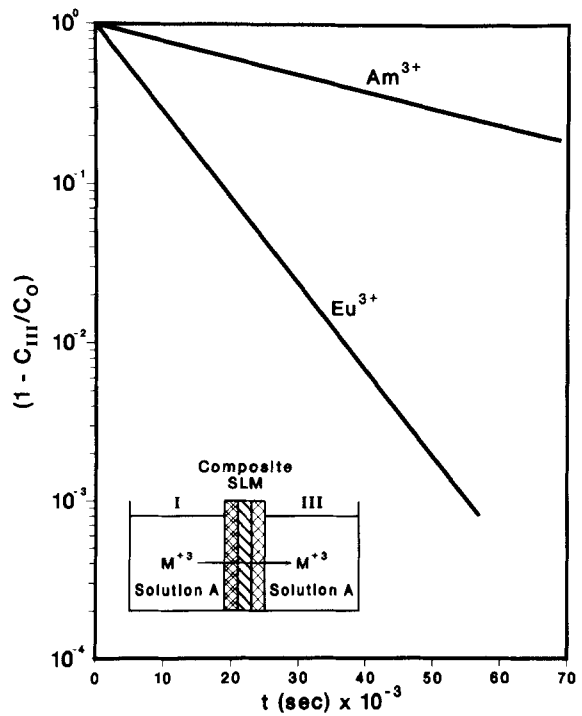

FIG. 22. Semilogarithmic plot of the concentration in Compartment I as a function of time (s) for the permeation of Eu^{3+} and Am^{3+} through the composite SLM of Fig. 21. The data are plotted as a function of the concentration increase in Compartment III, C_{III}, normalized to the initial concentration in Compartment I, C_0.

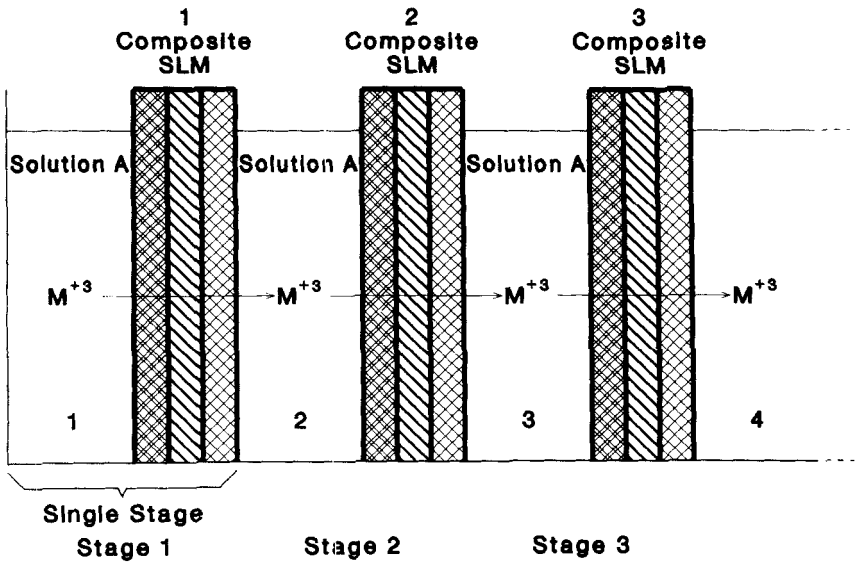

FIG. 23. Schematic description of a permeation process utilizing three identical composite SLMs in series.

SLMs of area Q, the permeation rate constants k_i of the metal cation, present at low concentration levels, through each composite SLM are identical and equal to

$$k = P(\text{SLM(A)})\frac{Q}{V} \tag{18}$$

The concentration variation in the ith compartment, C_i, with time will then be given by the equation (*23*)

$$C_i = C_0 \frac{(kt)^{i-1}}{(i-1)!} \tag{19}$$

where C_0 is the initial concentration in Compartment 1 at time zero. Equation (19) holds for the following initial condition $t = 0$, $C_1 = C_0$, C_2, C_3, $C_4, \ldots = C_i = 0$. The concentration in the final compartment C_F is given by

$$C_F = C_0 - \Sigma_i C_i \tag{20}$$

Equations (19) and (20) can be used to calculate how the concentrations of Eu^{3+} and Am^{3+} vary with time in a separation which makes use of several composite SLMs. The results of such a calculation, performed for nine identical membranes, are shown in Fig. 24. Only the curves describing the Eu^{3+} concentrations in Compartments 1, 4, 7, and 10 have been drawn to avoid overcrowding. The concentration of Am^{3+}, when 90% of the initial Eu^{3+} has been recovered in Compartment 10, is also reported for comparison. After the nine-stages process, only 5% of the initial Am^{3+} is present together with Eu^{3+} as compared to 40% for the single-stage process. The long tails of the C_i vs time curves are caused by the equal values of the rate constants for each stage. They can be reduced, by suitably scaling the k values of the various stages, through the adjustment of the aqueous volume and the membrane area in the various compartments. In this case Eqs. (19) and (20) are not any longer valid and a more complicated mathematical procedure has to be used to solve the set of differential equations which

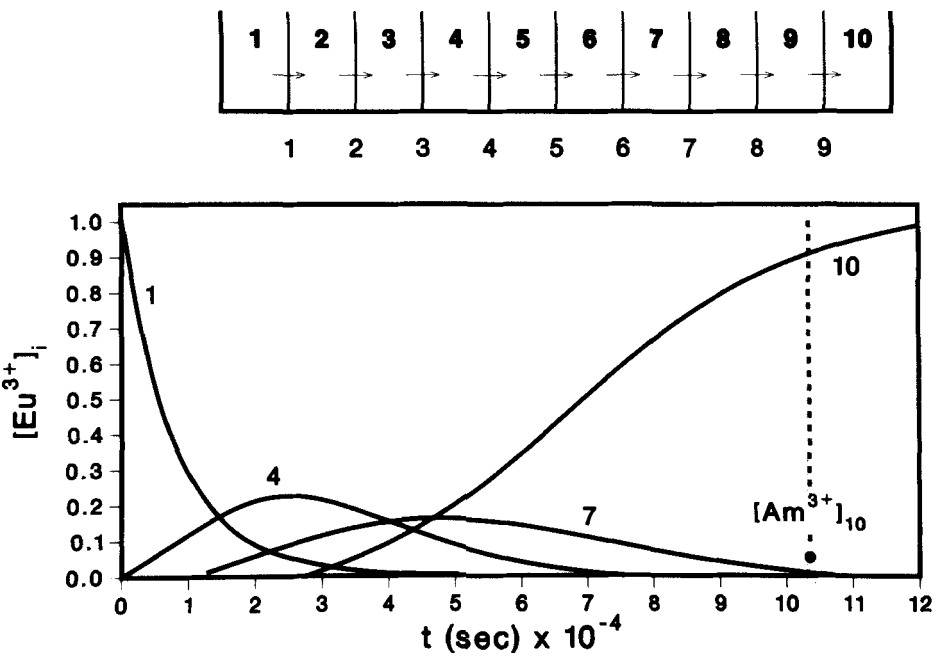

FIG. 24. Concentration of Eu^{3+} vs time (s) in Compartments 1, 4, 7, and 10 in a multistage permeation process of Eu^{3+} utilizing nine identical SLMs separating 10 aqueous compartments having equal volumes. $[Eu^{3+}]_i$ is the concentration in the ith compartment normalized to the concentration at time zero in Compartment 1. The solid circle indicates $[Am^{3+}]_{10}$.

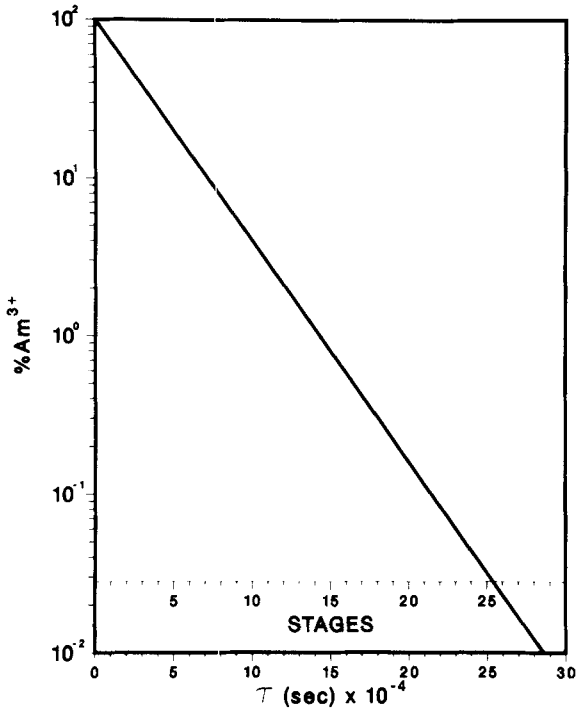

FIG. 25. Fraction of initial Am^{3+}, % Am^{3+}, which is accompanying Eu^{3+} as a function of the number of stages used to perform the separation. The straight line is calculated for a 90% recovery of the initial Eu^{3+}. τ is the time required to recover 90% of the initial Eu^{3+}.

describe the process. When $k(Eu^{3+})$ and $k(Am^{3+})$ are constant, Eqs. (19) and (20) can be also used to calculate the number of stages which are required to recover a fixed amount of Eu^{3+} in presence of a given amount of Am^{3+}. The results of such a calculation are shown in Fig. 25. The straight line of Fig. 25 represents the percentage of initial Am^{3+} which is accompanying Eu^{3+}, as a function of the number of stages, for a 90% recovery of the initial Eu^{3+}. From Fig. 25 it follows that the number of stages required to recover 90% of the initial Eu^{3+} in the presence of 1, 0.1, or 0.01% of the initial Am^{3+} is equal to 14, 21, and 29, respectively. The abscissa also shows the time, τ, required to recover 90% of the initial Eu^{3+} at a given degree of purity. This time is a function of the membrane area over volume ratio of the experimental apparatus used for the separation. It can be contracted or expanded by performing the separation with higher or lower values of the term Q/V.

Therefore, from what we have reported above, it appears that composite SLMs can offer a possibility of bypassing the single-stage limitations of SLM separations. The specific nature of each composite SLM is a function of the nature of the metal species which have to be separated. By taking advantage of the variety of aqueous complexing agents and of membrane carriers which are available, suitable composite SLMs can be devised for many different separation purposes. Although the design of separation cascades utilizing composite SLMs seems relatively simple when dealing with very dilute solutions of metal species, the same is presently not true when concentrated metal solutions are involved. With concentrated metal solutions appreciable composition variations can take place in the aqueous phases during the permeation. Therefore, suitable and practical ways of keeping the driving force of the permeation process constant, by continuous addition of chemicals without rendering the system too complicated, must be devised.

CONCLUSIONS AND SLM LIFE-TIME

The studies performed in our laboratory have led us to the development of models which suitably describe the rate-determining phenomena occurring in the permeation of metal species through SLMs. As a result of these models, simple equations have been derived which describe in a quantitative way the permeability of SLMs to metal species for a wide range of concentrations in terms of a few, simple, and often independently measurable parameters. These equations take into account the chemistry of the system as well as the hydrodynamics and geometrical parameters which characterize a SLM permeation process. The equations hold for both flat-sheet and hollow-fiber SLMs when relatively high linear flow velocities of the aqueous streams are used. The validity of the derived models and corresponding equations has been successfully tested on several SLM systems, utilizing a variety of membrane carriers and metal species. By using the derived permeability equations, simple mathematical expressions have also been obtained for the separation factor which characterizes a SLM separation. In this way it is possible to make good predictions of the extent of separation that can be achieved by using a SLM and how the separation is going to be affected by the concentration and hydrodynamic parameters which describe the system.

When metal species having very similar chemical behavior have to be separated, the use of a single SLM is not sufficient to obtain clean separations because of the single-stage limitation of the process. In this case composite SLMs, consisting of two complementary SLMs sandwiching a suitable aqueous solution, can be used in series to perform a multistage separation. By using composite SLMs interposed between compartments

TABLE 5
Membrane Density, Investment, and Operating Costs of Membrane Modules of a Different Type

Module type	Membrane surface per module volume (m^2/m^3)	Investment cost	Operating cost
Tubular	25–50	High	High
Plate and frame	400–600	High	High
Hollow fiber	600–1200	Low	Low

containing identical aqueous electrolyte solutions, very clean separations are in principle always obtainable, providing the number of stages is sufficiently large.

As far as the shape of the SLM is concerned, hollow-fibers seems to be the most convenient shape of membrane support to be used for practical purposes. Hollow-fibers represent a very attractive solution to the need of operating membranes with very high throughputs. As indicated in Table 5, which refers to membrane modules designed for reverse osmosis, hollow-fiber SLM modules can have packaging densities as high as 1000 m^2/m^3. This value compares to about 500 m^2/m^3 for plate and frame and to about 50 m^2/m^3 for tubular membrane modules. Moreover, hollow-fiber SLM modules should be characterized by low investment and operating cost because of the reduced hardware and favorable hydrodynamics which minimize aqueous concentration polarization effects and membrane fouling. A typical industrial size hollow-fiber SLM module is shown in Fig. 26. Modules of this type could be utilized, for example, for the removal of actinides from aqueous nuclear wastes using the SLM system reported in

TABLE 6
Parameters of a Conceptual SLM Process for the Removal of Am^{3+} and Other Actinides from an Acidic Nuclear Waste. The SLM System is Described in Fig. 16

Volume 20,000 L
Pumping rate 3.5 gpm
Linear flow velocity 14.5 cm/s
Re 103 (laminar flow)
$P(Am^{241}) = 1 \times 10^{-3}$ cm/s

$$\ln\frac{C}{C_0} = -\frac{Q}{V}Pt$$

20 modules remove 99.9% of Am^{241} from 2×10^4 L in 24 h
Space occupied (modules, pumps, tubes, etc.) 1.5 $m^3 \approx 54$ ft^3

Fig. 16. Assuming a processing volume of 2×10^4 L/d, only 20 modules would be sufficient to remove 99.9% of the Am^{241}. The process could be particularly attractive considering the small volume occupied by the modules and that space is at a premium in nuclear operations where shielding and remote control devices are required. Some of the parameters characterizing such a conceptual process are summarized in Table 6.

From what we have shown so far, it appears that SLMs can represent a viable technology for the separation of metal species in solution. The basic phenomena which occur in SLMs separation processes are sufficiently well understood to permit the scale-up of laboratory units to industrial sized ones in many cases. The major uncertainty in the use of SLMs for industrial separation processes resides on the very little information presently available on SLM stability. Scattered and sometimes contradictory results have been obtained on the life-time of SLMs, ranging from a few days to several months. As pointed out also in Ref. *11*, we believe that probable causes of membrane instability can be (a) loss of extractant by solubility in adjacent aqueous solutions, (b) progressive wettability of the support pores induced by the lowering of the organic–water interfacial tension which results from the surface-active nature of many carrier molecules, and (c) the differential pressures existing between the inside and the outside of the SLM caused by the pumping of the solutions when hollow-fiber SLMs are used. Our preliminary studies on the stability of SLMs have indicated that the life-time of SLMs containing acidic carriers, such as HDEHP, is lowered when one of the aqueous solutions has high pHs. Since the water solubility of these carriers increases at high pHs, this observation is in agreement with (a). No

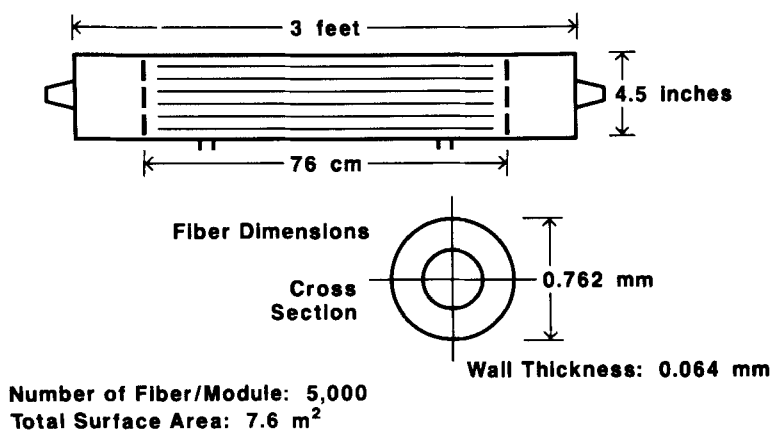

FIG. 26. Schematic representation of an industrial size hollow-fiber SLM module.

detailed or quantitative measurements have been performed on cause (b). Nevertheless, our experience with carriers which are very strong surfactants, such as alkylaryl sulfonic acids and long-chain quaternary alkylammonium salts, has indicated that within a few hours the organic phase can be displaced from the support pores and replaced with water. The same phenomenon was not observed with the weaker surface-active carriers OϕD[IB]CMPO, TOPO, and TLA. These observations are in agreement with (b). Finally, as far as cause (c) is concerned, we have observed that SLM life-times at least as long as 2 months can be obtained with Accurel polypropylene hollow-fiber SLMs containing tridodecylamine in *n*-dodecane as carrier, when the outside and inside hydraulic pressures are balanced. The result of such a stability test is shown in Fig. 27 where the rate of transport of H^+ ions through the SLM was measured. The experiment was run continuously using a single hollow-fiber SLM module of the type shown in Fig. 5, operated in a recycling mode. The hollow-fiber was 15 cm long, had a radius of 0.086 cm, and was operated at a flow rate of the feed solution equal to 20 cm^3/min. This corresponds to 8.22×10^4 fiber volumes per day. The feed solution was $[HNO_3] = 0.01\ M + [NaNO_3] = 1.0\ M$ and the strip solution was $[NaOH] = 0.1\ M + [NaNO_3] = 1\ M$. The stability of the SLM was measured by continuously monitoring the H^+ concentration in the feed solution by glass electrode potentiometry. Each experimental point corre-

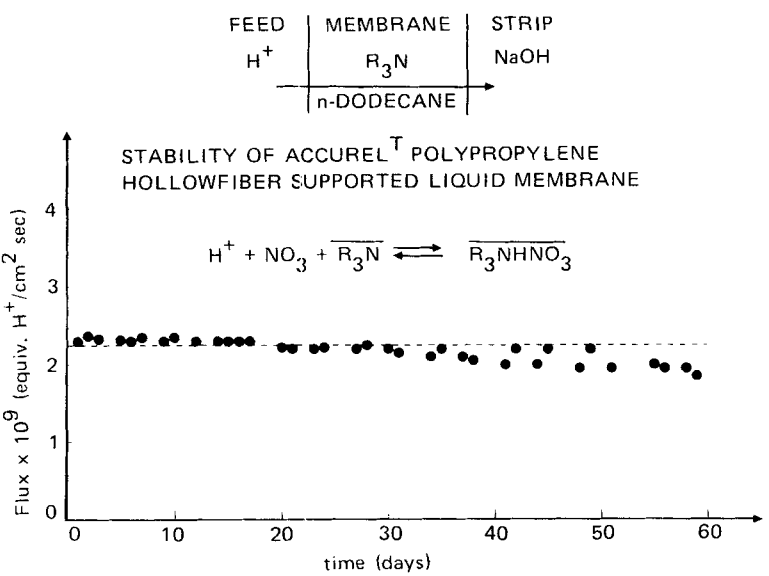

FIG. 27. Flux vs time (days) plot for a stability test of a single hollow-fiber SLM. R_3N = tridodecylamine.

sponds to a new feed solution. Between each replacement of the feed solution with a fresh one, the depleted feed kept on circulating through the hollow fiber. The reported membrane flux is an average flux, evaluated from the total H^+ equivalents which had crossed the membrane when the H^+ concentration had dropped from 10^{-2} to 10^{-4} *M*. The data reported in Fig. 27 show that during the 2 months of operation the average flux decreased to about 20% of the initial value while about 5×10^6 membrane volumes were treated. When the experiment was interrupted, the SLM was still working satisfactorily. These results, which compare with the value of 5×10^4 membrane volumes previously obtained by Pearson (*11*), look very encouraging for industrial use when one considers that intermittent or continuous reimpregnation of the support with the organic phase does not seem to present any difficulty. Presently more research efforts have been undertaken in our laboratory to obtain a deeper insight into the basic phenomena which control the stability of SLMs. At the same time, new techniques for the stabilization of the carrier in the membrane support will be experimented.

Acknowledgments

The helpful cooperation of R. Chiarizia, C. Cianetti-Pierce, E. P. Horwitz, L. Reichley-Yinger, P. G. Rickert, and V. Violante received during the development of the works herein reviewed is gratefully acknowledged.

This work was performed under the auspices of the Office of Basic Energy Sciences, Division of Chemical Sciences, U.S. Department of Energy, under contract number W-31-109-ENG-38.

REFERENCES

1. R. Bloch, in *Membrane Science and Technology* (J. E. Flin, ed.), Plenum, New York-London, 1970, pp. 171–187.
2. E. L. Cussler and D. F. Evans, *Sep. Purif. Methods, 3*, 399 (1974).
3. E. L. Cussler, *Multicomponent Diffusion*, Elsevier, Amsterdam, 1976, Chap. 8.
4. H. K. Lonsdale, *J. Membr. Sci., 10*, 81 (1982).
5. R. Marr and A. Kopp, *Int. Chem. Eng., 22*, 44 (1982).
6. J. D. Way, R. D. Noble, T. M. Flynn, and E. D. Sloan, *J. Membr. Sci., 12*, 239 (1982).
7. R. W. Baker, M. R. Tuttle, D. J. Kelly, and H. K. Lonsdale, *Ibid., 2*, 213 (1977).
8. W. C. Babcock, R. W. Baker, E. D. Lachapelle, and K. L. Smith, *Ibid., 7*, 71 (1980).
9. W. C. Babcock, R. W. Baker, E. D. Lachapelle, and K. L. Smith, *Ibid., 7*, 89 (1980).
10. W. C. Babcock, R. W. Baker, J. W. Brooke, D. J. Kelly, E. D. Lachapelle, and H. K. Lonsdale, NTIS, PB81-179947.
11. D. Pearson, in *Ion Exchange Membranes* (D. S. Flett, ed.), Society of Chemical Industry, London, 1983, pp. 55–73.

12. P. R. Danesi and R. Chiarizia, *Crit. Rev. Anal. Chem., 10*, 1–126 (1980).
13. P. R. Danesi, E. P. Horwitz, G. F. Vandegrift, and R. Chiarizia, *Sep. Sci. Technol., 16*, 201 (1981).
14. P. R. Danesi, E. P. Horwitz, and P. Rickert, *Ibid., 17*, 1183 (1982).
15. R. Chiarizia, A. Castagnola, P. R. Danesi, and E. P. Horwitz, *J. Membr. Sci., 14*, 1 (1983).
16. P. R. Danesi, C. Cianetti, and V. Violante, *Ibid., 14*, 175 (1983).
17. P. R. Danesi, R. Chiarizia, and A. Castagnola, *Ibid., 14*, 161 (1983).
18. P. R. Danesi, E. P. Horwitz, and P. G. Rickert, *J. Phys. Chem., 87*, 4708 (1983).
19. P. R. Danesi, C. Cianetti, and E. P. Horwitz, *Solv. Extr. Ion Exch., 1*, 299 (1983).
20. C. Cianetti and P. R. Danesi, *Ibid., 1*, 565 (1983).
21. P. R. Danesi, *J. Membr. Sci., 20*, 231 (1984).
22. P. R. Danesi and C. Cianetti, *Ibid., 20*, 201 (1984).
23. P. R. Danesi and C. Cianetti, *Ibid., 20*, 215 (1984).
24. P. R. Danesi, E. P. Horwitz, P. G. Rickert, and R. Chiarizia, International Symposium on Actinide-Lanthanide Separations, ACS Meeting, Honolulu, Hawaii, December 16–22, 1984.
25. P. R. Danesi, L. Reichley-Yinger, C. Cianetti, and P. G. Rickert, *Solv. Extr. Ion Exch., 2*, 781 (1984).
26. E. P. Horwitz, H. Diamond, and D. Kalina, in *Plutonium Chemistry* (W. T. Carnall and G. Choppin, eds.), ACS Symposium Series No. 216, 1983, pp. 433–450, and references therein.
27. E. P. Horwitz, H. Diamond, D. Kalina, L. Kaplan and G. W. Mason, *Proc. Int. Solv. Exch. Conf. ISEC'83*, Denver, Colorado, August 26–September 2, 1983, pp. 451–452, and references therein.
28. P. R. Danesi, "Separation by Supported Liquid Membrane Cascades," U.S. Patent Application and Assignment, DOE Case S-59, 617, August 1983.